

# Instalación para el estudio de la propagación de ondas de presión en conductos y su aplicación en túneles para trenes de alta velocidad

## *Experimental set-up for the study of pressure waves propagation in ducts and its application in tunnels for high speed trains*

Félix Sorribes Palmer\*, Oscar López García

Universidad Politécnica de Madrid (UPM)

---

### Resumen

Se ha construido una instalación experimental de bajo coste para realizar ensayos a escala de la onda de compresión que se generan en el interior de un túnel al introducirse en él un tren a alta velocidad, con el fin de estudiar posibles configuraciones para reducir la presión de la onda reflejada en la salida. El coeficiente de reflexión de varias terminaciones ha sido medido y la influencia de la porosidad en la salida ha sido evaluada utilizando el método de la pulsoreflectometría acústica.

Palabras clave: ondas de presión, trenes de alta velocidad, túnel

### Abstract

*A low-cost experimental facility has been built to perform scale measurements of the pressure waves generated by a high speed train entering inside a tunnel, in order to study possible configurations to reduce the pressure reflected back at the tunnel exit. The reflection coefficient of some tunnel terminations has been measured and the influence of the porosity at the exit has been evaluated by using the Acoustic Pulse Reflectometry method (APR).*

*Keywords: pressure waves, high speed trains, tunnel.*

---

## 1. Experimental set-up for the study of pressure waves propagation in ducts and its application in tunnels for high speed trains

### Nomenclature

$\alpha$  Attenuation constant of the pressure waves inside the duct

$\eta$  Dynamic viscosity of the air,  $kg \cdot m^{-1} \cdot s^{-1}$

$f$  Frequency, Hz

$\omega$  Sound pulsation,  $rad \cdot s^{-1}$

$\rho$  Air density,  $kg \cdot m^{-3}$

$\Delta p_{fr}$  Increase in pressure due to friction effects caused by the entry of the main part of the train into the tunnel, Pa

$\Delta p_{HP}$  Drop in pressure caused by the passing of the train head at the measurement position in the tunnel, Pa

$\Delta p_N$  Increase in pressure caused by the entry of the nose of the train into the tunnel, Pa

\*Email autor de contacto: felix.sorribes@upm.es

$\Delta p_T$	Drop in pressure caused by the entry of the tail of the train in the tunnel, $Pa$
$A$	Cross-sectional area of the tunnel, $m^2$
$a$	Inner radius of the cylindrical PVC, $m$
$A_0$	Cross-sectional area of the train, $m^2$
$c_0$	Speed of sound in the air, $m \cdot s^{-1}$
$\gamma$	Heat capacity ratio of the air
$\kappa$	Thermal conductivity, $w \cdot m^{-1} \cdot K^{-1}$
$cp$	Specific heat at constant pressure
$Pr$	Prantdl number
$Fe$	Scale factor between the microphones
$k$	Wave number, $m$
$Zc$	Characteristic impedance of cylindrical duct, $kg \cdot m^{-2} \cdot s^{-1}$
$D$	Tunnel diameter, $m$
$M$	Mach number
$q$	Volumetric velocity inside the tube
$R$	Reflection coefficient at the duct end
$U$	Train speed, $m \cdot s^{-1}$
$\sigma$	Perforated duct porosity

## Introduction

In order to introduce the work done in this article has been considered necessary a review of the researches done in high speed train's aerodynamics, specially related with pressure waves generated when the train is passing through a tunnel. The rapidly varying changes in pressure due to high speed train entering a tunnel and their reflections at the discontinuities in the tunnel can cause discomfort to the passengers.

When the train approaches the tunnel entrance the air inside the tunnel begins to be compressed due to the open-air local field preceding the train nose. When the head of the train reaches the tunnel entrance the pressure increases faster until the nose is completely inside the tunnel, this interaction between the entrance hood and the train nose determines the shape of the compression wave, but the total increase in pressure is  $\Delta p_N$ . The pressure continues increasing slowly due to the viscous effects on the tunnel wall and the train surface, until the end of the train reaches the tunnel entrance, and an expansion wave is generated  $\Delta p_T$ . The pressure decrease suddenly  $\Delta p_{HP}$  when the train nose passes the measurement point. The train reference signature defined by the standard EN14067-5:2006:E is shown in figure 1.

A good review of state of the art on the aerodynamic and aeroacoustic problems of high-speed railway train and the strategies to alleviate undesirable effects is made in Raghunathan et al. (2002). Raghunathan explains the influence in the quality of comfort, the safety of the passengers and the environment of the train's

aerodynamic drag, pressure variations inside train, train-induced flows, cross-wind effects, ground effects, pressure waves inside tunnel, impulse waves at the exit of tunnel, noise and vibration and the energy consumption. In it are also compiled some expressions to estimate: the train's aerodynamic drag, the pressure jumps of the compression wave generated at the entrance when the train enters into a tunnel and also the impulsive micro-pressure wave (MPW) which is radiated outside when the compression wave reaches the tunnel exit.

The aerodynamic phenomena during the entering of the train into the tunnel were treated theoretically in Hara (1961). The compression wave transient and its reflections in the tunnel during the train going through it are studied numerically in Zeng and Gretler (1995). A theoretical model for the pressure field in a tunnel generated by an entry of a travelling train modeled by a pair of moving monopoles into a semi-infinitely long tunnel is presented in Sugimoto and Ogawa (1997), the model is validated with CFD solving directly the Euler equations for inviscid and compressible gas.

An analytical investigation of the compression wave generated by a different train entering a tunnel and the influence in the wave shape of the train nose geometry is done at Howe (1997a). In this analytical solution the train is modeled by a uniformly translating continuous distribution of monopole sources whose density is proportional to the local gradient of the cross-sectional area of the train. The head wave is expressed as the convolution product of the sources and an acoustic Green's function whose determination is simplified at low Mach numbers, when the characteristic thickness of the head wave is large compared to the tunnel diameter. Also a second dipole of comparable strength is attributed to 'vortex sound' sources in the shear layers of the black-flow out of the tunnel of the air displaced by the train. The initial profile of the wavefront of the compression wave is determined principally by the train velocity, the blockage ratio, which is the ratio of the cross section area of the train and tunnel, the nose profile of the train, the shape of the tunnel entrance and the environment. The influence of the Mach number ( $M=U/c_0$ ) is studied in Howe (1997b) and the models are validated with the published experimental measurements presented by Maeda et al. (1993).

The effect of vents in the tunnel entrance portal in order to increase the rise time of the wave to alleviate the impulsive micro-pressure wave at the tunnel exit is analyzed in Howe (1998) and Howe (1999a). The maximum compression wave rise time that can be obtained with vents is equal to the time of passage of the front of the train through the perforated section. The Rayleigh's method for the approximate calculation of potential flow from the open end of a semi-infinite flanged cylinder is applied in Howe (1999b) to obtain analytical representations of the Green's function describing the generation of sound waves within a flanged cylinder by sources located in the neighborhood of the open end.

The pressure rise across the wave front  $\frac{\rho U^2}{1-M^2} \frac{A_0}{A} \left(1 + \frac{A_0}{A}\right)$  is given approximately in Howe et al. (2000). The amplitude of this pressure is typically 1-3% of the atmospheric pressure (around 150 dB) when the train Mach number exceeds about 0.2 (at 250 km/h). In this article is demonstrated that a "flared" portal entrance hood without windows behaves as an ideal hood producing a linear increase in pressure with distance across the wavefront, with a constant pressure gradient that is as small as practicable, but also implies a great increase in construction costs and space requirements.

The aerodynamic phenomena by a train traveling at high speed through a long tunnel is analyzed by means of quasi one-dimensional numerical simulation in Baron et al. (2001), in several tunnel configurations in order to establish tunnel design criteria for long-range underground high-speed railways, also the positive and negative effects of pressure relief ducts and partial air vacuum are discussed.

A reduce-scale (1/77) experimental set-up to study the compression wave generation is done in Bellenoue et al. (2002) and is validated with 3-D simulation, and with full-scale test published measurements. The generated compression wave is clearly established as planar wave after it has propagated four times the tunnel diameter inside the tunnel, and the 3-D model can be replaced by a 2-D (axially symmetric) model, saving this computational time. The optimal longitudinal cross section area distribution of the train nose, in order to increase

the rise time of the compression wave in the tunnel, can be deduce using axially symmetrical models, while drag and aerodynamic stability optimization in open air should be realized by means of 3-D models.

The resistance coefficients of the train from full scale measurements inside tunnel during routine operation were calculated in Vardy and Reinke (1999). In Bourquin et al. (2002) measurements of the propagation of pressure waves in a tube were undertaken and the change on shape due to unsteady viscous effects, as skin friction and heat transfer thanks to the length of the facility (112.3 m).

A theoretical analysis of the influence of the unvented hood geometry on the wavefront and its optimal size can be found in Howe et al. (2003a), and the optimal distribution and size of the windows in a vented hood is studied in Howe (2003b). The infrasound generated when a axisymmetric model of a train enters along the axis of a duct is studied in Howe (2003c). This low-frequency pressure pulses generated by the train entering and leaving the tunnel, so-called tunnel continues waves (TCW), is studied again in Kikuchi et al. (2009), also an interesting method of separation of incident wave from pressure data measured in tunnel is presented.

The influence of the train nose profiles in the generation of the wavefront is studied in Sato and Sassa (2005) numerical, together with an experimental set-up used to validate the results. The thickness of the wavefront can be made many times larger than its typical thickness order of 5 tunnel diameters  $D$ , when the wave is reflected at a tunnel exit with a discrete distribution of rectangular windows as shown in Howe and Cox (2005). The expansion wavefront reflected at the exit and the expansion wave caused by the inward propagating pulses generated at the windows are shown for a uniform and a linear 10 windows area distributions. A detailed analysis of the wave radiated from the portal reveals that cumulative nonlinear effects of propagation over long distances make little or no contribution to free space radiation of the micro-pressure wave. A compact algorithm that permits 'real-time' design studies of the compression wave generated by a train passing through a double-track tunnel entrance hood and the analytical model is validated with experimental results is formulated in Howe et al. (2006). This algorithm permits the designer to isolate the different contributions to the compression wave: the interactions of the train nose with the hood portal, the junction between the hood and the tunnel, the effect of the windows, and the contribution of the separated flow along the sides of the train. A genetically optimized tunnel-entrance hood (dimensions and distribution and sizing of the hood windows) is studied in Howe (2007) in order to reduce the maximum pressure gradient.

A method based on the signature of the pressure waves during their propagation inside the tunnel, required low CPU cost is presented in William-Louis y Tournier (2005). This method only predicts pressure changes but not the air temperature or velocity, and is only valid for simple tunnels (without cross-section changes, airshafts, etc...).

In Iida et al. (2006) an analytical method based on the aeroacoustic theory developed by Howe is applied to a short "acoustically compact" hood having a window on its side wall, and the boundary element method is used for calculating the potential flow through a portal of arbitrary geometry. A parametric analysis and an experimental study is performed in order to show the great influence of the relative length of the train nose to the distance between the window and the hood entrance in the performance of the hood. Another parametric numerical study of the micro-pressure wave is done in Kaoua et al. (2006).

The flow generated by train in a tunnel with side branches is studied in William-Louis and Tournier (1998). A method to predict the sound field in long enclosures with side branches is proposed in Liu, and Lu, (2009), the model proposed is validated with experiments, and with an acoustic modeling program ODEON. Field measurements and numerical simulation performed on the distortion of the compression wave generated by a train entry, and its propagation through a slab track with inclined side branches (with orifice-shaped apertures at the junction) tunnel is done in Fukuda et al. (2006). In Ricco et al. (2007) is also studied numerically an experimentally the pressure wave generated in the tunnel during the passing by of a high speed train

Numerical simulations of the flow field around high speed trains passing by each other inside a tunnel are done in Fujii and Ogawa (1995), Hwang and Lee (2000) and Hwang et al. (2001).

The pressure waves reflect at tunnel discontinuities such as changes in cross-sectional area, chimneys, airshafts, side branches and also every time that a wave finds the train. This multiple reflections can create localized regions where constructive interferences produces much higher pressure that can also affect to passengers and personnel within the tunnel.

A study of the sonic boom generated at the tunnel exit when the compression wave reaches the exit and a review of some passive and active alleviation methods is presented in Vardy (2008). The compression wave and the micro-pressure wave generated for a different hoods (linear horn, discontinuous, equal and enlarged cross-section with and without windows and gradient hood), using 3-D numerical simulations and moving-model experiments is presented in Liu et al. (2010). The optimal shape of the hood in order to diminish the micro-pressure wave is studied in Murray and Howe (2010).

The amplitude of the micro-pressure wave that emerges from the tunnel end is proportional to the gradient of the compression wave at the exit. In long tunnels (more than 3 km length) with modern concrete slab track the non-linear steepening progressively reduces the compression wave thickness, increasing the disturbance radiated from the tunnel end, which becomes similar in strength to a sonic boom. A ballasted track can be regarded as an effective porous sound absorbing material in the low-frequency range.

Two new methods for the prediction of the micro-pressure wave are proposed in Yoon and Lee (2001), the first method combines acoustic monopole analysis (generation of compression wave) and the method of characteristics (wave propagation inside tunnel) with the Kirchhoff formulation (computation of a micro-pressure wave), and the second method replaces the first two stages by 2D-3D Euler/Navier-Stokes solvers. In this article is concluded that the combined acoustic monopole analysis/method of characteristics-Kirchhoff formulation is very useful tool for preliminary design.

Most of the experimental set-ups launch an asymmetric train model through horizontal circular cylindrical pipe using a driving wheel, an air compressed chamber, or an elastic bundle. In Kim et al. (2003) is studied numerically and experimentally the distortion of a compression wave reflected from a baffled open end of a shock tube, the incident expansion wave is generated by a sudden rupture of a diaphragm.

This article is focused on the influence of the shape of the exit in the pressure that is reflected back inside the tunnel. For studying the reflection coefficient we have used a speaker to generate the pressure wave instead of using a scale train model projected at high speed along the axis of the duct. This fact extremely reduces the cost of the experimental setup, however just a part of the problem can be studied.

The reflected energy into the conduit can be determined by calculating the energy radiated outward. The study of acoustic radiation at the end of a circular unflanged duct without thickness, for a symmetric excitation is discussed in Levine and Schwinger (1948). This publication presents an analytical solution, valid for the frequency range in which acoustic waves inside the duct can be considered planes. In Norris and Sheng (1989) the acoustic radiation at the end of an infinite circular flanged duct is analyzed theoretically and approximated formulas are proposed for the reflection coefficient for a flanged and unflanged duct. The influence of the shape of the duct end on the pressure waves is analyzed experimental and numerically in Dalmont et al. (2001). In Selamet et al. (2001) different exits are analyzed numerically with the Boundary Element Method (BEM).

The effect of the radius of curvature of the extreme nonlinear losses is discussed in Atig et al. (2004) with the TMTC. The APR and TMTC method, outlining the advantages and disadvantages of each one are compared in Lefebvre et al. (2007). The acoustic pulse reflectometry does not require calibration since only a microphone is needed, although requires very long lines which makes it less portable installation than the installation TMTC, meanwhile with the TMTC method is easier to measure the impedance at high frequencies, but requires multiple microphones and precise calibrations increase the time of tuning the facility. Silva et al. (2009) proposed approximate formulas for the reflection coefficient of the flange and unflanged duct. The porous side walls have been previously studied in Nishimura and Ikeda (2008), comparing their efficiency in reducing the reflection coefficient at the end of the conduit for pressure waves of low frequency.

## Theoretical analysis

The equation of linearized pressure wave propagation in a perfectly smooth and rigid insulated conduit (Kinsler et al. (2000), Flecher and Rossing (1991)) is

$$\nabla^2 p - \frac{1}{c_0^2} \frac{\partial^2 p}{\partial t^2} = 0, \quad (1)$$

where the instantaneous pressure  $p$ , inside the cylindrical tube depends on the distance to the sound source  $x$ , on the distance to the longitudinal axis of the duct  $r$ , on the angle of the point position with the horizontal axis  $\varphi$ , on speed of sound in the medium  $c_0$ , and on time  $t$ . Assuming axial symmetry, the solution of equation (1) is

$$p(r, x, t) = \sum_{m=-\infty}^{m=+\infty} \sum_{n=0}^{n=+\infty} c_{mn} J_m \left( \frac{q_{mn} r}{a} \right) e^{i(k_{mn} x - \omega t)}, \quad (2)$$

$p(x=0, r, \varphi, t) = f_\omega(r, \varphi) e^{-i\omega t}$  where  $J_m$  is the Bessel function of first kind and the coefficients  $c_{mn}$  are obtained using the initial condition applying the orthogonality properties of Bessel functions, finally the coefficients are

$$c_{mn} = \frac{1}{\pi a^2} \frac{q_{mn}^2}{(q_{mn}^2 - m^2) J_m^2 \left( \frac{q_{mn} r}{a} \right)} \int_0^{2\pi} \int_0^a f_\omega(r, \varphi) J_m \left( \frac{q_{mn} r}{a} \right) e^{-im\varphi} r dr d\varphi. \quad (3)$$

The propagation mode  $(m, n)$  of an acoustic disturbance that propagates axially along the duct depends on the wave number  $k_{mn} = \sqrt{(\omega/c)^2 - (q_{mn}/a)^2}$ . The first propagation mode of the disturbance is a plane wave  $K_{00} = (\omega/c)$ , in which there are not traversal displacements. The condition of propagation of an acoustic mode is that the wave number must be real  $K_{mn}$ , otherwise the wave will decay exponentially and this is known as an evanescent wave. The lowest zero of the Bessel function is  $q_{11} = 1.8412$ , therefore the cut off frequency is

$$f_c = \frac{\omega_c}{2\pi} = \frac{1.8412c}{a} \frac{1}{2\pi}. \quad (4)$$

Four diameters inside the tube from the sound field is primarily unidimensional and the equation (1) can be written as

$$\frac{\partial^2 p}{\partial x^2} - k^2 \frac{\partial^2 p}{\partial t^2} = 0, \quad (5)$$

where  $K = (\omega/c_0)$  is the wave number and  $p(x, t) = \text{Re}\{Ae^{ik(ct-x)} + Be^{ik(ct+x)}\}$  is the acoustic pressure inside the tube ( $A$  and  $B$  are complex quantities). In a sinusoidal sound field the particle velocity is

$$u(x, t) = -\frac{1}{i\omega\rho} \frac{\partial p}{\partial x} = \frac{1}{\rho c} (Ae^{ik(ct-x)} - Be^{ik(ct+x)})$$

It should be noticed that when is just a wave traveling in the  $x$  direction  $B=0$ . The volumetric velocity  $q$  is the integral of the velocity of the particles  $u$  (homogeneous and uniform) in the cross section  $S$  of the duct  $q = \int_S u dS = Su$ . If standing waves are propagating inside the duct, the acoustic impedance is the ratio between the sound pressure and the volume rate

$$Z(x) = \frac{p}{q} = Z_c \frac{Ae^{-ikx} + Be^{ikx}}{Ae^{-ikx} - Be^{ikx}}, \quad (6)$$

where  $Z_c = \rho c/S$  is the characteristic impedance of cylindrical duct. If the plane at  $x=0$  is defined as the input plane or reference, the impedance at this level can be called input impedance  $Z_e$  is

$$Z_e = \frac{p(0)}{q(0)} = Z_c \left[ \frac{A+B}{A-B} \right]. \quad (7)$$

At a distance  $x=L$  the impedance is

$$Z_L = \frac{p(L)}{q(L)} = Z_c \left[ \frac{Ae^{-ikL} + Be^{ikL}}{Ae^{-ikL} - Be^{ikL}} \right]. \quad (8)$$

The reflection coefficient at the end ( $x=0$ ) is the relationship between the amplitudes of the reflected wave between the incident

$$R = \frac{B}{A} = \frac{Z - Z_c}{Z + Z_c} = \frac{\bar{Z} - 1}{\bar{Z} + 1}. \quad (9)$$

If the wall is almost rigid ( $\bar{Z} \gg 1$ ) there is a phase reflection ( $R=1$ ), and if the impedance is very small ( $\bar{Z} \ll 1$ ) reflection is almost in antiphase ( $R=-1$ ).

## Experimental set-up

If the pressure waves which propagate inside the duct find a discontinuity, part of the wave energy is transmitted in the forward direction of the wave and part is reflected back. To analyze the amount of energy that is reflected in the discontinuity, the effective pressure of the incident wave is compared with the effective pressure of the reflected wave. This ratio, between the effective pressure (root mean square of the instantaneous pressure amplitude  $p(t)$ ) of the reflected wave  $P_{efRW}$  and the effective pressure of the incident wave  $P_{efIW}$  is called reflection coefficient  $R$  at the duct end

$$R = \frac{P_{efRW}}{P_{efIW}}. \quad (10)$$

The experimental set-up consists in a wave generator which sends an electric pulse which is reproduced in a high speaker that is situated in one end of the PVC cylindrical tube of length  $L_c=5\text{m}$ , inner radius  $a=0,0284\text{m}$  and thickness  $e=3.10^{-3}\text{m}$ . The sound inside the tube is captured by two microphones, this data is send to the computer were is postprocesed. Temperature and humidity are also registered. The equipment used in the experimental set-up in the scale tests is detailed at the table 1 and a scheme of the facility is shown in the figure 2. The first cutoff frequency is approximately 3500 Hz. The frequency of study has two limitations, a lower one due to the laboratory length, and a higher one due to the ability of the speaker reproduce the signal without too much distortion.

The frequency of the pressure wave that represents the rise up of the wavefront generated by a high speed train entering a tunnel is calculated from keeping the Helmholtz number ( $H=k.r$ ). Therefore the relation between the frequency at full scale and test scale is proportional to ratio between the inner radius of the tunnel and the inner radius of the duct.

The attenuation constant of the pressure waves inside the duct is evaluated and some measurements are done in order to validate the results obtained with the experimental set-up with the results published in the bibliography (Silva et al. (2009), Levine and Schwinger (1948), Baron et al. (2001)).

### Propagation constant of the plane waves inside the duct

The formula proposed by Flecher and Rossing (1991) to calculate the attenuation constant  $\alpha$  of the pressure waves inside a cylindrical pipe, where the law of exponential attenuation is assumed ( $P=P_0e^{(-\alpha x)}$ ) where  $x$  is the distance traveled by the wave, is

$$\alpha \approx \frac{w}{c_0} \left( \frac{1}{r_v \sqrt{2}} + \frac{\gamma-1}{r_t \sqrt{2}} \right), \quad (11)$$

where  $r_v$  is the dimensionless parameter that takes into account the corrections due to the viscous boundary layer and  $r_t$  is the dimensionless parameter that takes into account the corrections due to the thermal boundary layer and its expressions are

$$r_v \approx 632.8a\sqrt{f}(1-0.0029(T_0-300)), \quad (12)$$

$$r_t = r_v Pr^{1/2} = r_v \left( \frac{\eta c_p}{\kappa} \right)^{1/2} \approx 532.2a\sqrt{f}(1-0.0031(T_0-300)). \quad (13)$$

Losses due to wall vibrations of the tube have been neglected because it is rigid enough for the level of pressure that is being used.

Substituting in the above equations the conditions under which measurements have been performed ( $a=0.0284$  m,  $T_0=297$  K and  $P_0=94768$  Pa) and taking into account the corrections of the table 2 the attenuation constant obtained is  $\alpha=0.0331$ .

To evaluate experimentally the attenuation constant of the pressure wave inside the tube due to the interaction between the air inside and the walls measurements were made with microphones located in different regions of the duct, and then their positions were exchanged and re-measured.

To relate the measurements between microphones should be known the scale factor  $F_e$ , which is defined as the ratio of effective pressure measured at the microphone M2 and the effective pressure measured at the microphone M1 ( $F_e = P_{efM2}/P_{efM1}$ ). To obtain the scale factor and the attenuation constant, 3 measures were made with the microphones M1 located at 3000 and M2 at 4000 mm of the high speaker ( case a), subsequently the position of microphones was exchanged and performed other 3 measures ( case b). Dividing in both cases the pressure at the microphone M2 between the pressure at the microphone M1 and dividing them, the attenuation coefficient  $\alpha$  can be calculated

$$\frac{\left. \frac{P_{M2}}{P_{M1}} \right|_a}{\left. \frac{P_{M2}}{P_{M1}} \right|_b} = e^{(-2\alpha x)}, \quad (14)$$

as well as the scale factor  $F_e$

$$\frac{\left. \frac{P_{M2}}{P_{M1}} \right|_a}{\left. \frac{P_{M2}}{P_{M1}} \right|_b} = F_e^2. \quad (15)$$

The results of measurements made at different distances between the microphones ( $s = |x_{M2} - x_{M1}|$ ) are shown in the table 3.

It is convenient to note that the attenuation constant is proportional to the square of frequency, and the error in its calculation can lead to errors in the reflection coefficient of about 2% for large distances (3 m). To avoid such errors the method of the two microphones and four calibrations (TMFC) Hendrie (2007) could be used, where it is not necessary to determine the propagation constant.

## Validation of the experimental setup with referenced cases

### Flanged and unflanged duct

The results for the reflection coefficient at the end of a cylindrical duct for the cases of flanged and unflanged terminations which are shown in the figure 3, were obtained by using a burst of 3 cycles and frequencies between 700 and 1500 Hz. In this figure they are compared with the values obtained with the formulas proposed in the literature (Silva et al. (2009); Levine and Schwinger (1948)). From them it follows that the measurements are acceptable and that the facility is appropriate. The flange at the end of the duct decreased significantly the intensity of the reflected wave into the tube (approximately 9%) at this frequency.

### Chimneys as pressure reliefs

In order to validate the experimental setup have been also tested the pressure that is transmitted through a chimney of different cross section area  $S_h$  and the pressure reflected to the tube of cross section area  $S_c$ . The length of the chimney has been chosen in order to be able to distinguish the incident and the reflected waves in the time domain signals recorded in the microphones. The pressure transmitted through the chimney has been evaluated with the ratio between the effective pressure wave transmitted through the chimney,  $p_{efOTH}$  and the effective pressure of the incident wave at the junction between tube and the chimney,  $p_{efOI}$  ( $r_{ITH} = p_{efOTH}/p_{efOI}$ ).

Transmission coefficients obtained in the chimney tests, multiplied by the cross sectional area are compared with those provided by the literature (Baron et al. (2001)) in the figure 4, in which it can be seen that the accuracy of the experimental set up is acceptable.

## Results

Due to the porosity of the nozzle the incident wave is partially reflected at each hole creating a new wave that sums in antiphase with the incident and rest of the reflected waves in the other holes, with a time delay proportional to the distance between the holes.

Reflection coefficient has been measured varying the number of open holes in the porous nozzle, closing one by one the hole starting from the furthest from the exit (also the smallest). The results shown in the table 4 indicate that the number of holes has a strong influence in the intensity of the reflected wave which varies from 60% when they are all open to 80% when they are all closed. The fact that closing the last hole slightly decreases the ratio of reflected wave may be due to interference between the hole and the opening of the exit, because the waves generated in both discontinuities do not behave as a plane wave.

Open holes through the surface are a high pass filter that reflects the waves and transmits low-frequency waves whose frequency is above the cutoff frequency of the hole that following Flecher and Rossing (1991) is  $f_c = 0.011c \left(\frac{b}{a}\right) \sqrt{\frac{l}{sl}}$ . Where  $t$  is the thickness of the tube,  $l$  is the effective acoustic length of the hole and  $2s$  is the distance between holes. In the porous side wall the frequencies of the holes starting with the smallest would be 305, 408, 447, 466, 485 and 505 Hz, all the holes reflect and transmit the incident wave. In contrast, if the holes are closed up a low pass filter for waves that propagate along the duct.

To study the effect of porosity on the duct wall (size and distance between holes) regardless of the energy radiated in the exit duct, a duct section has been perforated and located between two lines long enough to avoid reflections at the end, and has evaluated the energy reflected and transmitted in this section. The porous section has 60 holes of diameter 12 mm, distributed in 3 rows of 10 (separated 20mm) on each side of the plane of symmetry.

The influence of the porosity  $\sigma$ , has been analyzed by varying the number of holes  $\sigma = 0, 3, 7, 15 \%$  for a 3 cycles sinusoidal burst frequency of 1000 Hz and the energy reflected with the porous section is compared with the case in which the inside of the duct is completely smooth. The reflection coefficient obtained through the porous tube is defined as

$$T[\text{dB}] = 20 \log \left( \frac{\left| \frac{p_{it}}{p_{i\sigma}} \right|}{\left| \frac{p_{it}}{p_i} \right|} \right) \quad (16)$$

The results obtained which are shown in the table 5; indicate that the wave is practically reflected back as an open end termination when the porosity is large

## Conclusions

This study indicates that experimental set-up is adequate to evaluate the reflection coefficient at a duct end, the pressure transmitted through a chimney, and the transmission coefficient in a porous section.

The porous nozzle is an efficient system to decrease the coefficient of reflection of pressure waves that reach the outlet of the cylindrical duct. The porosity may increase by 20 % the efficiency of the bevel tip in reducing the intensity of the reflected wave and generate a more dispersed wave, which reduces the intensity of the transmitted wave outside. Also the chimney is an efficient method to reduce the pressure inside the duct, and optimizing the length in relation to the signal shape could decrease even more the pressure gradient and reduce the micro-pressure waves. The flange at the end of the duct can duplicate at high frequencies the power radiated out of the tube.

## Acknowledgments

The authors would like to acknowledge the support of Ineco.

## References

- [1] Atig, M., Dalmont, J., & Gilbert, J. (2004). Termination impedance of open-ended cylindrical tubes at high sound pressure level. *Comptes Rendus Mecanique*, 332:299–304.
- [2] Baron, A., Mossi, M., & Sibilla, S. (2001). The alleviation of the aerodynamic drag and wave effects of high-speed trains in very long tunnels. *Journal of Wind Engineering and Industrial Aerodynamics*, 89(5):365–40.
- [3] Bellenoue, M., Morinière, V., & Kageyama, T. (2002). Experimental 3-d simulation of the compression wave, due to train-tunnel entry. *Journal of Fluids and Structures*, 16(5):581 – 595.
- [4] Bourquin, V., Gillieron, C., & Monkewitz, P. (2002). Experimental analysis of the propagation of pressure waves in tubes. *TRANSAERO: A European Initiative on Transient Aerodynamics for Railway System Optimization*, 79.

- [6] Dalmont, J., Nederveen, C., & Joly, N. (2001) Radiation impedance of tubes with different flanges: numerical and experimental investigations. *Journal of Sound and Vibration*, 244(3): 505–534.
- [7] EN14067-5:2006:E, . Railway applications - Aerodynamics - Part 5: Requirements and test procedures for aerodynamics in tunnel.
- [8] Flecher, N. & Rossing, T. (1991). *Physics of musical instruments*. Springer-Verlag New York.
- [9] Fujii, K. & Ogawa, T. (1995). Aerodynamics of high speed trains passing by each other. *Computers & Fluids*, 24(8):897 – 908.
- [10] Fukuda, T., Ozawa, S., Iida, M., Takasaki, T., & Wakabayashi, Y. (2006) Distortion of compression wave propagating through very long tunnel with slab tracks. *JSME International Journal Series B Fluids and Thermal Engineering*, 49(4):1156–1164.
- [11] Grégoire, R., Réty, J., Kageyama, T., Bellenoue, M., & Morinière, V. (1997). Experimental study (scale 1/70) and numerical simulations of the generation of pressure waves and micro-pressure waves due to high-speed train-tunnel entry. *Proceedings of the 9th International Symposium on*
- [12] *Aerodynamics and Ventilation of Vehicle Tunnels*, pages 877–903.
- [13] Hara, T. (1961). Aerodynamic force acting on a high speed train at tunnel entrance. *The Japan Society of Mechanical Engineers*.
- [14] Hong Liu, T., Qi Tian, H., & Feng Liang, X. (2010). Design and optimization of tunnel hoods. *Tunnelling and Underground Space Technology*, 25(3):212 – 219.
- [15] Howe, M.S. (1997a). The compression wave produced by a high-speed train entering a tunnel. *Proceedings of the Royal Society of London. Series A: Mathematical, Physical and Engineering Sciences*, 454(1974):1523–1534.
- [16] Howe, M.S. (1999a). Prolongation of the rise time of the compression wave generated by a high-speed train entering a tunnel. *Proceedings of the Royal Society of London. Series A: Mathematical,*
- [17] *Physical and Engineering Sciences*, 455(1983):863–878.
- [18] Howe, M.S. (1999b). On Rayleigh's computation of the "end correction", with application to the compression wave generated by a train entering a tunnel. *Journal of Fluid Mechanics*, 385:63–78, April.
- [19] Howe, M.S. (2003b). Design of a tunnel-entrance hood with multiple windows and variable cross-section. *Journal of Fluids and Structures*, 17(8):1111 – 1121.
- [20] Howe, M.S., Iida, M., Fukuda, T., & Maeda, T. (2000). Theoretical and experimental investigation of the compression wave generated by a train entering a tunnel with a flared portal. *Journal of Fluid Mechanics*, 46:111–132.
- [21] Howe, M.S., Iida, M., & Fukuda, T. (2003a). Influence of an unvented tunnel entrance hood on the compression wave generated by a high-speed train. *Journal of Fluids and Structures*, 17:833–853.
- [22] Howe, M. (1997b). Mach number dependence on the compression wave generated by a high-speed train entering a tunnel. *Journal of Sound and Vibration*, 46:147–163.
- [23] Howe, M. (1998). The compression wave generated by a high-speed train at a vented tunnel entrance. *Acoustical Society of America*.
- [24] Howe, M. (2003c). On the infrasound generated when a train enters a tunnel. *Journal of Fluids and Structures*, 17(5):629 – 642.

- [25] Howe, M. (2007). The genetically optimized tunnel-entrance hood. *Journal of Fluids and Structures*, 23 (8):1231 – 1250.
- [26] Howe, M. & Cox, E. (2005). Reflection and transmission of a compression wave at a tunnel portal. *Journal of Fluids and Structures*, 20(8):1043 – 1056.
- [27] Howe, M., Iida, M., Maeda, T., & Sakuma, Y. (2006). Rapid calculation of the compression wave generated by a train entering a tunnel with a vented hood. *Journal of Sound and Vibration*.
- [28] Hwang, J. & Lee, D.H. (2000) Unsteady aerodynamic loads on high speed trains passing by each other. *Journal of Mechanical Science and Technology*, 14:867–878.
- [29] Hwang, J., Yoon, T.S., ho Lee, D., & gab Lee, S. (2001) Numerical study of unsteady flowfield around high speed trains passing by each other. *JSME International Journal Series B Fluids and Thermal Engineering*, 44(3):451–464.
- [30] Iida, M., Kikuchi, K., & Fukuda, T. (2006). Analysis and experiment of compression wave generated by train entering tunnel entrance hood. *JSME International Journal Series B Fluids and Thermal Engineering*, 49(3):761–770.
- [31] Kaoua, J.N., Pope, C.W., Henson, D.A., & Mott MacDonald Ltd, UK, . (2006). A parametric study into the factors affecting the development and alleviation of micro-pressure waves in railway tunnels. 12th International Symposium on Aerodynamics and Ventilation of Vehicle Tunnels.
- [32] Keefe, D. (1984). Acoustical wave propagation in cylindrical ducts transmission line parameter approximations for isothermal and nonisothermal boundary conditions. *Acoustical Society of America Journal*, 75:58–62.
- [33] Kikuchi, K., Ozawa, S., Takami, H., & Iida, M. (2009). Continuous pressure wave generated by a train running in a tunnel. *Journal of low frequency noise, vibration and active control*.
- [34] Kim, H., Lee, D., Kashimura, H., & Setoguchi, T. (2003). Propagation characteristics of compression waves reflected from the open end of a duct. *Journal of Mechanical Science and Technology*, 17:718–72.
- [35] Kinsler, L., Frey, A., Coppens, A., & Sanders, J. (2000). *Fundamentals of Acoustics*. Wiley.
- [36] Lefebvre, A., Scavone, G.P., Abel, J., & Buckiewicz-Smith, A. (2007). A comparison of impedance measurements using one and two microphones. *ISMA*.
- [37] Levine, H. & Schwinger, J. (1948). On the radiation of sound from an unflanged circular pipe. *Phys. Rev.*, 73(4):383–406.
- [38] Liu, J.h.i.a..c.h.u.n. & Lu, P.C. (2009). Sound field prediction in long enclosures with branches: A combined method. *Applied Acoustics*.
- [39] Maeda, T., Matsumura, T., Iida, M., Nakatani, K., & Uchida, K. (1993). Effect of shape of train nose on compression wave generated by a train entering tunnel. *The Japan Society of Mechanical Engineers*.
- [40] Murray, P. & Howe, M. (2010). Influence of hood geometry on the compression wave generated by a high-speed train. *Journal of Sound and Vibration*, 329(14):2915 – 2927.
- [41] Nishimura, M. & Ikeda, K. (2008). Reduction of sound reflection coefficient at open duct end by using porous side wall. *Journal of Environment and Engineering*, 3(2):351–362.
- [42] Norris, A.N. & Sheng, I.C. (1989). Acoustic radiation from a circular pipe with an infinite flange. *Journal of Sound Vibration*, 135:85–93.

- [44] Raghunathan, R.S., Kim, H.D., & Setoguchi, T. (2002). Aerodynamics of high-speed railway train. *Progress in Aerospace Sciences*, 38(6-7):469 – 514.
- [45] Ricco, P., Baron, A., & Molteni, P. (2007). Nature of pressure waves induced by a high-speed train travelling through a tunnel. *Journal of Wind Engineering and Industrial Aerodynamics*.
- [46] Sato, T. & Sassa, T. (2005). Prediction of the compression pressure wave generated by a high-speed train entering a tunnel. *International Journal of Computational Fluid Dynamics*, 19:53–59.
- [47] Selamet, A., Ji, Z.L., & Kach, R.A. (2001). Wave reflections from duct terminations. *Acoustical Society of America Journal*, 109:1304–1311.
- [48] Silva, F., Guillemain, P., Kergomard, J., Mallaroni, B., & Norris, A.N. (2009) Approximation formulae for the acoustic radiation impedance of a cylindrical pipe. *Journal of Sound and Vibration*.
- [49] Sugimoto, N. & Ogawa, T. (1997). Acoustic analysis of the pressure field in a tunnel, generated by entry of a train. *Proceedings: Mathematical, Physical and Engineering Sciences*.
- [50] Vardy, A.E. & Reinke, P. (1999). Estimation of train resistance coefficients in tunnels from measurements during routine operation. *Proceedings of the Institution of Mechanical Engineers, Part F: Journal of Rail and Rapid Transit*, 213.
- [51] Vardy, A. (2008). Generation and alleviation of sonic booms from rail tunnels. *Proceedings of The Ice-Engineering and Computational Mechanics*, 161:107–119.
- [52] William-Louis, M. & Tournier, C. (2005). A wave signature based method for the prediction of pressure transients in railway tunnels. *Journal of Wind Engineering and Industrial Aerodynamics*.
- [53] William-Louis, M. & Tournier, C. (1998). Non-homentropic flow generated by trains in tunnels with side branches. *International Journal of Numerical Methods for Heat & Fluid Flow*.
- [54] Yoon, T. & Lee, S. (2001). Efficient prediction methods for the micro-pressure wave from a high-speed train entering a tunnel using the kirchhoff formulation. *Journal of the Acoustical Society of America* 110(5):2379–2389.
- [55] Zeng, S.m. & Gretler, W. (1995). Pressure wave propagation in a short tunnel caused by passing trains. *Forschung im Ingenieurwesen*.
- [56] Hendrie D. A. (2007). Development of Bore Reconstruction Techniques Applied to the Study of Brass Wind Instruments.

Appendix A.

A.1. Figures

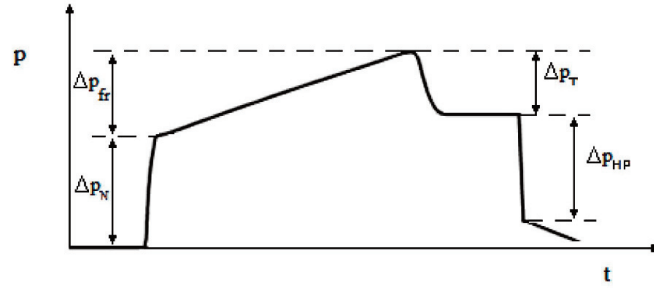


Fig. 1. Train reference signature defined by the standard UNE-EN 14067-5:2006

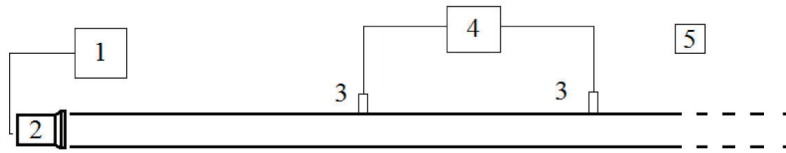


Fig. 2. Scheme of the facility components: wave's generator (1), high speaker (2), microphones (3), computer (4) and temperature and humidity sensor (5)

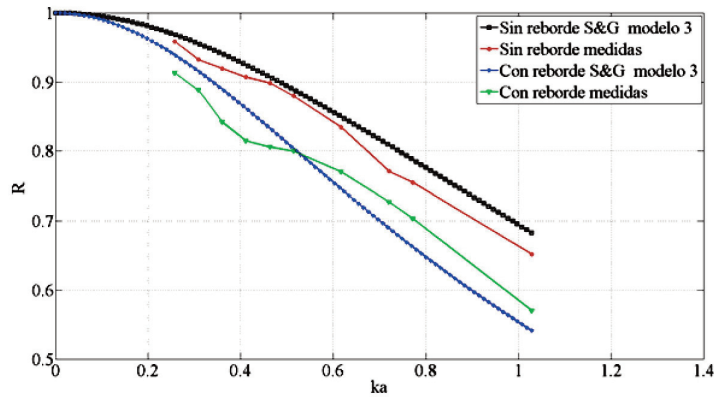


Fig. 3. Comparison of experiment results for the reflection coefficient  $R$  of a flanged and an unflanged duct with model 3 from Silva et al. (2009)

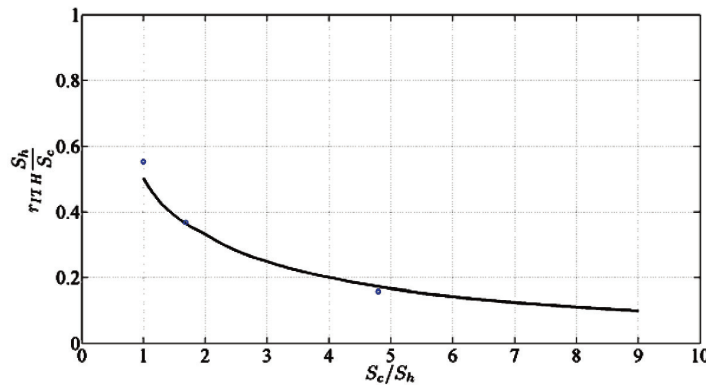


Fig. 4. Variation with the area ratio  $Sc/Sh$  of effective pressure transmitted by the chimney and the incident  $rITH$  multiplied by the inverse of the area ratio. Continuous line: results of Baron et al. (2001), circles: measurements.

A.2. Tables

Equipment	Model
Waves generator (1)	HP 33120A
High speaker (2)	ALTEC lansing
Microphones (3)	Sitecom TC-221
Computer (4)	HP Pavilion dv6
Temperature and humidity sensor (5)	RS 212-124

Table 1. Equipment used in the scale tests

Variable	Temperature correction
$\rho$	$1.1769 \cdot 10^{-4} (1 - 0.00335 (T_0 - 300))$
$\gamma$	$1.4017 (1 - 0.0025 (T_0 - 300))$
$\eta$	$1.846 \cdot 10^{-5} (1 - 0.00335 (T_0 - 300))$
$Pr^{1/2}$	$0.8410 (1 - 0.0002 (T_0 - 300))$
$c_0$	$347.23 (1 - 0.00166 (T_0 - 300))$

Table 2. Temperature corrections in the air properties

$s [m]$	$Fe$	$\alpha$
1	$1.0557 \pm 0.0033$	$-0.0344 \pm 0.0013$
2	$1.0776 \pm 0.0014$	$-0.0300 \pm 0.0012$
2.5	$1.0781 \pm 0.0256$	$-0.0313 \pm 0.0019$

Table 3. Scale factor,  $Fe$ , attenuation coefficient,  $\alpha$ , inside the PVC tube for different distances between the microphones  $s$ .

$N$	$\sigma [\%]$	$\alpha$
6	15.4	$0.611 \pm 0.002$
5	15.0	$0.613 \pm 0.001$
4	14.1	$0.810 \pm 0.002$
3	13.1	$0.635 \pm 0.001$
2	12.1	$0.706 \pm 0.001$
1	10.9	$0.780 \pm 0.001$
0	9.6	$0.800 \pm 0.002$

Table 4. Variation of the reflection coefficient  $R$  at the porous nozzle with the number of open vents  $N$ .

$\sigma$ [%]	$TL$ [dB]
0	-0.36 $\pm$ 0.05
3	-10.39 $\pm$ 0.05
7	-17.13 $\pm$ 0.05
15	-20.48 $\pm$ 0.05

Table. 5. Transmission coefficient in the porous section